The Journal of Experimental Biology 200, 477–485 (1997)
Printed in Great Britain © The Company of Biologists Limited 1997
JEB0437

VASCULAR PERIPHERAL RESISTANCE AND COMPLIANCE IN THE LOBSTER *HOMARUS AMERICANUS*

JERREL L. WILKENS*,[1], GLEN W. DAVIDSON†,[1] AND MICHAEL J. CAVEY[1,2]

[1]*Department of Biological Sciences, The University of Calgary, 2500 University Drive NW, Calgary, Alberta, Canada T2N 1N4* and [2]*Department of Anatomy, The University of Calgary, 3330 Hospital Drive NW, Calgary, Alberta, Canada T2N 4N1*

Accepted 24 October 1996

Summary

The peripheral resistance to flow through each arterial bed (in actuality, the entire pathway from the heart back to the pericardial sinus) and the mechanical properties of the seven arteries leaving the lobster heart are measured and compared. Resistance is inversely proportional to artery radius and, for each pathway, the resistance falls non-linearly as flow rate increases. The resistance of the hepatic arterial system is lower than that predicted on the basis of its radius. Body-part posture and movement may affect the resistance to perfusion of that region. The total vascular resistance placed on the heart when each artery is perfused at a rate typical of *in vivo* flow rates is approximately 1.93 kPa s ml^{-1}. All vessels exhibit adluminal layers of fibrils and are relatively compliant at pressures at or below heart systolic pressure. Arteries become stiffer at pressures greater than peak systolic pressure and at radii greater than twice the unpressurized radius. The dorsal abdominal artery possesses striated muscle in the lateral walls. This artery remains compliant over the entire range of hemolymph pressures expected in lobsters. These trends are illustrated when the incremental modulus of elasticity is compared among arteries. All arteries should function as Windkessels to damp the pulsatile pressures and flows generated by the heart. The dorsal abdominal artery may also actively regulate its flow.

Key words: artery, cardiovascular system, Crustacea, lobster, elastic modulus, vascular resistance, histology, *Homarus americanus.*

Introduction

The open circulatory system of decapod crustaceans consists of a heart that pumps hemolymph into seven parallel arteries (see review by McLaughlin, 1983). These vessels are the unpaired anterior median artery (AMA), sternal artery (SA) and dorsal abdominal artery (DAA) and the paired anterior lateral arteries (ALAs) and hepatic arteries (HAs). Each artery branches variously, depending on the tissue supplied, until small arterioles discharge into endothelium-lined capillaries and/or unlined tissue lacunae (Lockhead, 1950; McMahon and Burnett, 1990). The capillary and lacunar diameters may be as small as vertebrate capillaries. In some organs, such as the central nervous system and antennary glands, the capillary density is high, whereas the segmental appendages and abdominal muscles are almost totally devoid of capillaries. Crustaceans do not possess veins, but rather hemolymph is collected into discrete sinuses (Greenaway and Farrelly, 1984). All returning hemolymph passes through either the gills or the branchiostegal sinus before being delivered back to the pericardial sinus surrounding the heart. In order to understand hemolymph distribution and the load placed on the heart, we need information on the resistance to flow and the mechanical characteristics of each vascular bed.

The first part of this study was to measure the resistance to fluid flow of each of the seven arterial systems. Except for estimates of the total vascular resistance (R_t), which can be derived from measurements of mean ventricular pressure and calculations of cardiac output ($\dot{V}_b$) (Burger and Smythe, 1953; McMahon and Wilkens, 1975), the resistance characteristics of individual arterial systems of the crustacean vascular system are not known. The equation for calculating the total resistance of a system composed of parallel resistances predicts that the total vascular resistance against which the heart must pump will be low and that this will facilitate the large mass-specific cardiac output of crustaceans (McMahon and Wilkens, 1983).

The second aspect of this study was to compare the structure and elasticity of each of the seven arteries, since all arteries in *Homarus americanus* superficially appear to have a similar simple structure. ‘Typical’ crustacean arteries, including those of the lobster, have an elastic layer adjoining the lumen and an endothelium surrounded by a collagen-fiber adventitia

*e-mail: wilkens@acs.ucalgary.ca.
†Present address: Department of Physiology and Anatomy, Massey University, Private Bag 11222, Palmerston-North, New Zealand.

(Shadwick *et al.* 1990; Davison *et al.* 1995). No muscle layers are present in most species, with the exception of portions of the DAAs in the lobster *Panulirus interruptus* (Burnett, 1984) and the prawn *Sicyonia ingentis* (Martin *et al.* 1989). Elastic tissue has been identified in the DAA of a prawn (Martin *et al.* 1989). The arteries should thus serve as 'capacitance' vessels (Milnor, 1990) which, by their compliance, would reduce the pulsatility of hemolymph flow from the heart (Windkessel damping). However, we can predict that the arteries themselves, other than possibly the DAA, would not contribute to differential hemolymph distribution among the various vascular beds since they do not contain diameter-regulating muscle that could control their individual resistances. The only information about the mechanical properties of crustacean arteries is from data on the elastic properties of the DAA of *H. americanus* and the ALA and SA of the crab *Cancer magister* (Shadwick *et al.* 1990).

Materials and methods

Lobsters (*Homarus americanus* Milne Edwards) weighing between 300 and 660 g were purchased from a commercial supplier and maintained in an artificial seawater system at 12 °C.

As soon as a lobster was removed from the holding tank, the pericardial sinus, ventricular and DAA pressures were measured while the animal was held in a seawater bath at 12 °C. To do this, a hole just large enough to admit a cannula tipped with a 21 gauge needle was drilled through the carapace at an appropriate position. By probing through a hole above or lateral to the heart, the pericardial sinus pressure dorsal or lateral to the heart was recorded. Ventricular pressure (P_{vent}) was next measured by advancing the needle until it penetrated the dorsal wall of the heart. The cannula was filled with Cole's saline (Cole, 1941), adjusted to pH 7.6, and connected to a Hewlett Packard 2678C/311A pressure transducer and amplifier.

Next, the hemolymph was replaced with ice-chilled saline. As no anti-clotting agents are known for crustacean hemolymph, the clotting reaction was slowed by gradually lowering the body temperature to 1 °C over an approximately 30 min period by burying the animal in crushed ice. While this temperature was maintained, the carapace over the heart was removed, and the heart was perfused with oxygenated ice-cold saline delivered at 5–10 ml min^{-1}. A second stream of cold saline was directed into the pericardial sinus. This caused venous hemolymph returning to the sinus to be washed into the holding tank. Post-operative examinations showed that little or no clotting had occurred in the arteries or in various hemolymph sinuses of the body.

Arterial resistance

Following exsanguination, the resistance of each arterial system was determined. The resistances measured represent the entire vascular pathway of each artery, from the origin of the artery to the return *via* the lacunae and sinuses to the pericardial sinus. This entire pathway is referred to as an arterial system or simply as an artery. Each artery was cannulated immediately adjacent to the heart. Back pressure to the perfusate was measured with a Gould P23Db Statham transducer from a T-junction side-arm placed close to the cannula tip. The cannula was tied into the artery, and the system was tested for leaks by observing the passage of a small quantity of Methylene-Blue-stained saline. The origins of the AMA, ALAs and DAA were visible without further dissection. The HAs and SA were accessed by opening the dorsal wall of the heart. A calibrated peristaltic pump was used to generate the flow. The resistance of the cannula tip was subtracted from arterial resistance measurements. Arteries were perfused with Cole's saline, adjusted to pH 7.6.

Arterial system resistance (kPa s ml^{-1}) to flow was calculated using the hydraulic resistance equation (Berne and Levy, 1992) where the pressure drop from the perfusion cannula to the pericardial sinus (kPa) is divided by flow rate (ml s^{-1}) produced by a peristalatic pump:

$$\text{arterial system resistance} = \frac{P_i - P_o}{\text{flow rate}}\ , \qquad (1)$$

where P_i is the perfusion pressure measured from a T-junction side-arm placed close to the cannula tip and P_o is the hydrostatic pressure in the pericardial sinus adjacent to the heart.

From the individual resistance values, it was possible to calculate the total vascular resistance (R_t, kPa s ml^{-1}) of the seven parallel arteries from the equation:

$$\frac{1}{R_t} = \frac{1}{R_1} + \frac{1}{R_2} + \dots \frac{1}{R_7}\ . \qquad (2)$$

Equation 1 was also used to estimate the R_t of the heart where P_i–P_o was replaced by the mean ventricular pressure and cardiac output was replaced by flow rate. Mean ventricular pressure (P_{vent}) was calculated from the equation for estimating mean arterial pressure (Berne and Levy, 1992; Reiber, 1994):

$$P_{vent} = P_d + T_s(P_s - P_d)\,, \qquad (3)$$

where P_s is peak systolic pressure, P_d is diastolic pressure and T_s is the systolic fraction of the beat cycle. The systolic fraction is close to 50 % of the cycle in resting lobsters.

The radii of unpressurised inflated arteries, taken adjacent to the heart, were measured using an ocular micrometer. The radius of a vessel was measured at the point where the transmural pressure just began to rise. Measurements of the radius calculated from the width of gently flattened arteries, as in Wilkens and McMahon (1994), were similar to those obtained by inflation.

Arterial elasticity

Apart from the AMA, the elasticity of all arteries was determined *in vitro*. Owing to difficulties in cannulating the AMA outside the animal, the elasticity of this small vessel was

tested *in situ*. To do this, an incision was made in the dorsal wall of the ventricle and the AMA was cannulated by inserting a saline-filled, hand-drawn polyethylene cannula into the artery through the valve at its origin from the heart. The cannula was secured with surgical silk. The other end of the cannula was connected to a saline-filled reservoir that could be moved vertically to alter the pressure head at the cannula tip. This pressure was measured as described above. The artery was tied off approximately 1 cm anterior to the cannula tip and was inflated by raising the reservoir slowly over a period of 5–10 min. A piece of black film was placed beneath the artery to facilitate measurement of the diameter by ocular micrometer.

For arteries other than the AMA, thread markers were glued to each artery *in situ*, and the distance between threads was measured. Each artery was then removed and stored in saline at 4 °C until used. To make measurements, each excised artery was placed in a saline bath and two cannulae, one connected to the saline reservoir and the other to the pressure transducer, were tied into opposite ends, and all visible side branches were tied off. While observing the thread markers, each artery was restretched to its *in situ* length. The artery was trans-illuminated, and the diameter was measured by ocular micrometer.

To measure wall thickness, and from this to calculate internal radius, arteries were fixed and processed for microtomy. Each artery was inflated to the point where the inflation pressure just began to rise from zero and then fixed at this length and pressure with 10 % formalin in saline and stored at 4 °C for histology. Vessels were processed concurrently to normalize the influence of dehydration, clearing and infiltration on specimen shrinkage. Arteries were embedded in paraffin, and sections (10 μm in thickness) were stained with Hematoxylin and Eosin.

The incremental modulus of elasticity (E_{inc}) is a measure of wall stiffness used to characterize the elastic behavior of tissues:

$$E_{inc} = \frac{2(1-v^2)Rr^2\Delta p}{(R^2-r^2)\Delta R}, \quad (4)$$

where v is Poisson's ratio taken to be 0.5 (Bergel, 1961), R is the external radius, r is the internal radius and p is pressure in kPa (Chandran, 1992). If the wall is incompressible, the terms (R^2-r^2) and $(1-v^2)$ are constant (Bergel, 1961). For a given Δp, an elastic vessel will show a greater ΔR and therefore a smaller value of E_{inc}; conversely, a stiff vessel will show a smaller ΔR and a higher E_{inc}.

Histology

To evaluate whether the walls of any of the arteries contained striated muscle fibers, lengths of arteries were cut open longitudinally and flattened, or in some cases teased apart, in saline under a coverslip. They were viewed with a Leitz Dialux microscope fitted with Smith differential interference-contrast optics.

For higher-resolution photomicrography, arteries were dissected from the body, pinned to dental wax in a Petri dish and flooded with primary fixative (2.5 % glutaraldehyde, 0.2 mol l^{-1} phosphate buffer at pH 7.4, and 0.14 mol l^{-1} sodium chloride). After 5 min, the arteries were cut into short cylindrical segments with razor blades, and the segments were transferred to fresh fixative for an additional 60 min at ambient temperature. Without rinsing, the segments were immersed in secondary fixative (2 % osmium tetroxide and 2.5 % bicarbonate buffer at pH 7.2) for 60 min in an ice-bath. Following a brief rinse with demineralized water, the specimens were dehydrated with a graded series of ethanol, transferred through propylene oxide, infiltrated, and embedded in LX-112 epoxy resin (Ladd Research Industries, Burlington, VT). Thin sections (1 μm in thickness) were cut with glass knives on a Sorvall MT-2B ultramicrotome and stained with an alkaline solution of Azure II and Methylene Blue (Richardson *et al.* 1960). The sections were viewed and photographed with a Nikon Optiphot compound microscope equipped with planachromatic objective lenses and an HFX-IIA photomicrographic attachment.

Statistics

Data are presented as means ± S.E.M. Data were compared statistically by paired *t*-test (α=0.05).

Results

Ventricular and sinus pressures

The ventricular and pericardial sinus pressures were measured in intact lobsters before they were prepared for arterial perfusion. The systolic and diastolic ventricular pressures were 1.62±0.19 and 0.52±0.09 kPa, respectively (N=14). The pulse pressure was 1.10±0.22 kPa. The mean ventricular pressure was 1.07 kPa (equation 3). The pericardial sinus pressure relative to the same level in the bath was 0.52±0.09 kPa. After the pericardial chamber had been opened dorsally, the ventricular pulse pressures were reduced by 50 % (N=3) and pericardial sinus pressure immediately fell to zero.

Resistance

The relationship between perfusion flow rate and back pressure taken from the DAA of six lobsters is shown in Fig. 1. Back pressure rose linearly with increases in perfusion rate, while the calculated resistance decreased non-linearly as an inverse decay function (equation 1). For direct comparisons among the arteries, the resistance of each of the arteries, except the AMA, was measured as they were perfused from 1 to a maximum of 10 ml min^{-1} (Fig. 2). It was only possible to perfuse the AMA at a maximum rate of 5 ml min^{-1} because it became greatly distended at higher perfusion rates. In all cases, resistance declined non-linearly as perfusion rate was increased.

The resistances of all arteries perfused at 2 ml min^{-1} and their unpressurized radii are shown in Fig. 3. The values for the ALAs and HAs represent the mean radius and resistance for these paired vessels. It is acknowledged that this flow rate

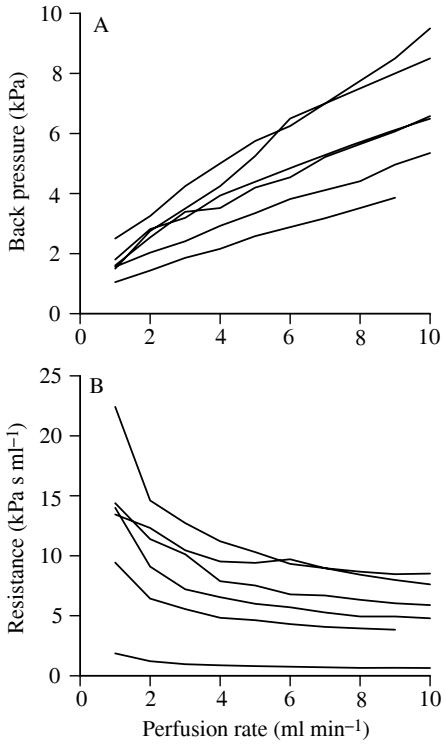

Fig. 1. Plots of the (A) back pressure and (B) resistance to perfusion of the dorsal abdominal artery in six lobsters.

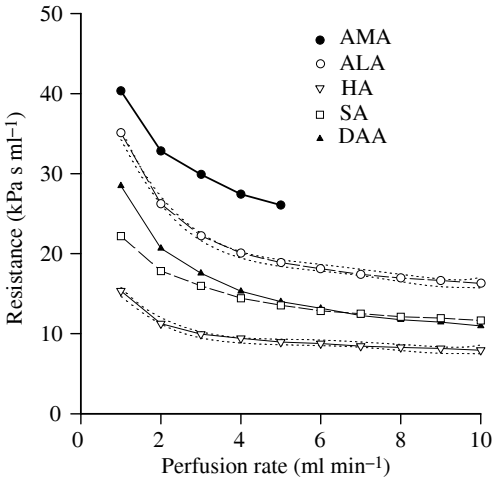

Fig. 2. Summary of the resistance of each artery type over a range of perfusion rates (N=9). The dotted lines surrounding the plots for the anterior lateral arteries (ALAs) and the hepatic arteries (HAs) are the 95 % confidence limits around the fourth-order regression line. AMA, anterior median artery; SA, sternal artery; DAA, dorsal abdominal artery.

(2 ml min^{-1}) is not the natural flow rate for any of these arteries in an intact lobster (Reiber, 1992); however, the total cardiac outflow at this rate would be 14 ml min^{-1}. This is close to the flow measured from vigorously beating, semi-isolated lobster hearts (10–15 ml min^{-1}) when all outflow was restricted to the SA (Wilkens *et al.* 1996). The radius of each artery at a point adjacent to the heart is presented in Table 1. A reciprocal relationship exists between resistance and radius for all arteries except the HA, where the resistance is lower than predicted by its radius. For *H. americanus*, Reiber (1992) measured the actual flow rate in all arteries except the HA by the pulsed Doppler technique (Table 1). After estimating the flow rates for the HAs (3.8 ml min^{-1}, 6.2 % of total arterial area), we calculated the passive resistance of arteries to perfusion at the same rate (by extrapolation). The R_t would be approximately 1.9 kPa s ml^{-1}.

The abdominal posture, extended and flexed, had a significant effect on the resistance to flow in the DAA when perfused at 2 ml min^{-1} (P<0.05, d.f. 12), but not at higher rates (Fig. 4). The resistance was 38–50 % higher when the abdomen was flexed than when it was extended. In three of seven preparations, there was no measured difference in resistance between these two positions.

Mechanical properties

The pressure–volume relationship for each artery over the pressure range 0–3.5 kPa is illustrated in Fig. 5. Recall that peak systolic pressure in intact lobsters is approximately 2 kPa. For each artery except the DAA, the volume increased rapidly at lower pressures, but in the range of 1.5–2.0 kPa the curves flattened out. The DAA continued to expand linearly over this range of pressures. The AMAs of three of seven animals were relatively non-compliant at all pressures, so in this and subsequent figures the data from these animals are plotted separately and labeled AMA′.

The radii of all arteries, except for the AMA′ of three animals, increased two- to 3.5-fold at transmural pressures of 2–3.5 kPa (Fig. 6). For the ALAs, HAs and SA, a transition from relatively compliant to stiff occurs at an arterial extension ratio between 1 and 2. This is seen as a flattening out of the radius extension ratio R/R_i, where R_i is the unpressurized radius. The DAA remained relatively compliant even when the radius had increased 3.5-fold. The distensibility of lobster arteries is impressive. In one animal, air was accidentally introduced into the DAA. Several attempts were made to dislodge it by increasing the perfusion rate to above 35 ml min^{-1} using the ‘prime’ function of the perfusion pump. The artery became inflated like a balloon during each attempt even though the air was not dislodged. The artery relaxed slowly to its original diameter over several minutes following each of the three inflations, but did not rupture.

The E_{inc} for the arteries is plotted against the radius extension ratio in Fig. 7. For the ALAs, HAs and SA, a transition from relatively compliant to stiff occurs at an arterial extension ratio between 1.5 and 2.5. The E_{inc} increased linearly with increasing pressure above this transition. The E_{inc} values for AMA again fell into two groups, with three animals possessing stiff walls (AMA′). The DAA remained relatively compliant even when the radius was increased 3.5-fold.

Table 1. *Measured values of* Homarus americanus *arterial dimensions and resistances to perfusion with saline*

Artery	Unpressurized radius (mm)	Area (mm^2)	Percentage of total area	Hemolymph flow rate (Reiber, 1992) ($ml\,min^{-1}$)	Resistance based on Reiber's data ($kPa\,s\,ml^{-1}$)	Approximate passive resistance to perfusion at rate equivalent to Reiber's data§ ($kPa\,s\,ml^{-1}$)
AMA	0.99	3.1	5.8	7.78	8.3	80.0
ALA (×1)† (×2)	1.50	7.1 (14.1)	13.3 (26.6)	0.57	112.6	17.1
HA (×1)† (×2)	1.30	3.3 (6.6)	6.2 (12.4)	(3.8)‡	(16.9)	10.5
DAA	2.15	14.5	27.2	12.6	5.1	10.2
SA	2.18	14.9	28.0	38.9	1.6	10.0
Total, based on all seven arteries		53.3	100.0			
R_t					0.93	1.93

Flow rates are those measured by Reiber (1992, his Table 3.3) and mean P_{vent} (1.07 kPa) is that measured in the present study. For the last column, the resistance was obtained by extrapolating the perfusion rates to the same flow rates measured by Reiber.

AMA, anterior median artery; ALA, anterior lateral artery; HA, hepatic artery; DAA, dorsal abdominal artery; SA, sternal artery.

†Single artery of pair for ALAs and HAs.

‡Based on the assumption that 6.2 % of the total arterial area will carry 6.2 % of the hemolymph.

§Values for the flow rates for the AMA, ALAs and HAs are taken from data used to prepare Fig. 2; the resistances of the SA and DAA were obtained by extrapolation to higher flow rates from the polynomial regression relationships for each artery.

Histology

The lining of a lobster artery consists of a deep, frequently multilayered endothelium (Fig. 8). Transmission electron micrographs reveal layers of cross-banded fibrils covering the apices of the endothelial cells and segregating them from the luminal contents (not shown). The fibrillar layer is thinnest in the DAA and thickest in the SA. It accounts for a considerably larger fraction of total wall thickness in the smaller arteries (ALAs, AMA and HAs) than in the larger vessels (SA and DAA). Fibroblastic cells are often interspersed with the endothelial cells.

The DAA is the only one of the arteries to contain striated muscle. Striations are evident in fresh arteries when viewed by differential interference-contrast microscopy, and they are especially prominent in thin histological sections for the bright-field microscope (Fig. 8F). Striated cells, restricted to the

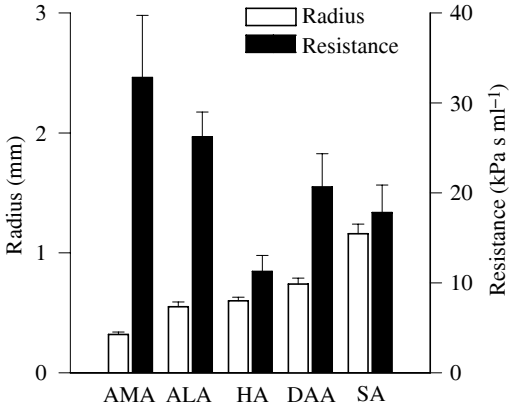

Fig. 3. Comparison of the unpressurized radius and the resistance to perfusion at 2 $ml\,min^{-1}$ for each artery type (N=4 for radius, N=9 for resistance). Values are mean + S.E.M. Abbreviations are explained in the legend to Fig. 2.

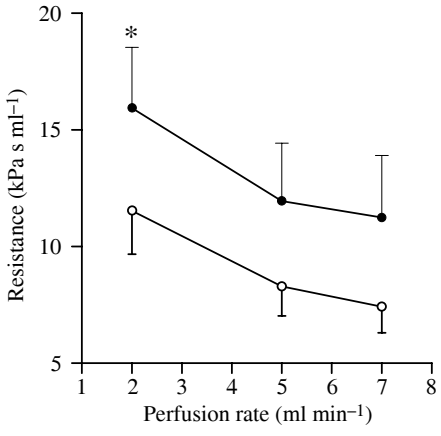

Fig. 4. Resistance measurements of the dorsal abdominal artery when the abdomen was passively extended (open circles) and flexed (filled circles) (N=7). Resistances were significantly different (P<0.05) at 2 $ml\,min^{-1}$ perfusion rate (asterisk). Values are mean ± S.E.M.

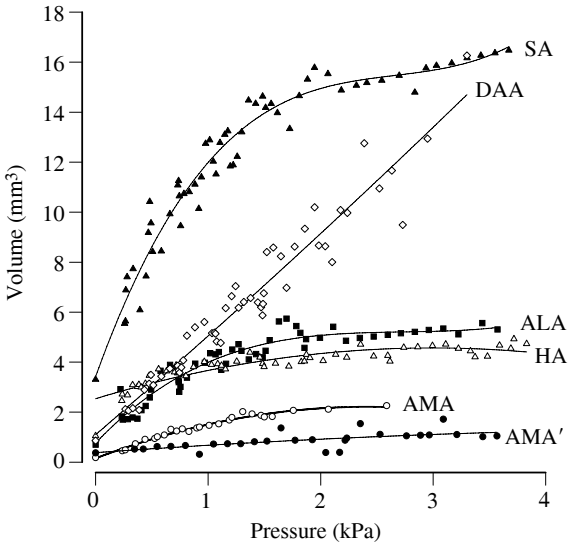

Fig. 5. The pressure–volume response, calculated from the internal radius, of each artery type taken adjacent to the heart. The lines are calculated using a second-order regression equation (N=3 for AMA′, N=5 for AMA, N=7 for all others). Abbreviations are explained in the legend to Fig. 2; AMA′, values for the three of the seven animals with a relatively non-compliant AMA at all pressures.

lateral walls of the DAA, may account for as much as 50 % of total wall thickness. The muscle cells are obliquely oriented, primarily in a circumferential orientation.

Discussion

The pressures measured from the pericardial sinus and heart define the physiological range of pressures at which the arteries operate in settled lobsters. These pressures are similar to those reported by Burger and Smythe (1953). The circulatory system, consisting of the heart, arteries and return sinusus, is pressurized, as is apparent from the mean pericardial sinus pressure of 0.52 kPa, and the pericardial sinus pressures are the lowest of any point in the animal's body (McMahon and Wilkens, 1983; Wilkens and Young, 1992). The peak transmural pressure of an artery during systole is expected to be slightly less than the ventricular pressure, because the pressures of sinuses around arteries are greater than that of the pericardial sinus. When the pericardial sinus is opened, the ventricular pulse pressure decreased by half, and pericardial sinus pressure immediately decreased to 0 kPa. The decrease in ventricular pulse pressure could result from a number of causes, including a reflex decrease in vascular resistance or a drop in afterload on the heart that ordinarily results from the pressurized vascular system (Wilkens and McMahon, 1994). This is mentioned to draw attention to the distinction between resistance to flow and afterload.

Resistance

As perfusion rate increases, the radius of each artery increases and the resistance decreases non-linearly. The curves

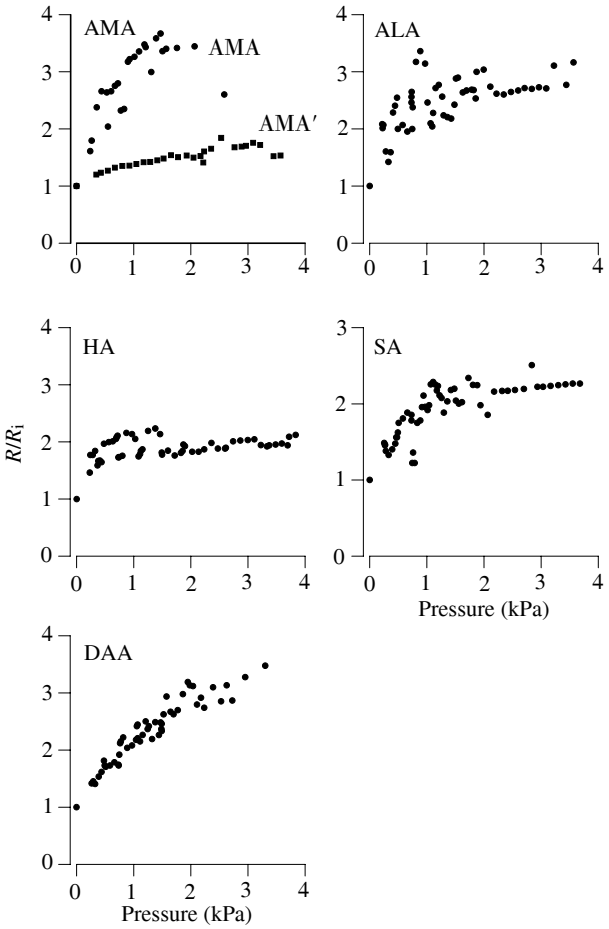

Fig. 6. The compliance of arteries expressed as the radius extension ratio (R/R_i) over a range of pressures (N as in Fig. 5). Abbreviations are explained in the legend to Fig. 2.

shown in Fig. 2 all fall within the 95 % confidence interval for a fourth-order regression equation, in agreement with the predictions of Poiseuille's Law that the resistance to flow will decrease as the fourth power of radius. The resistance also decreases non-linearly with increasing size of the artery. It is important to remember that resistance is proportional to vessel length. Preliminary observations of vessel length and branching patterns by corrosion casting of individual vessels indicate that the HAs may be shorter than the ALAs, which have a similar radius. If this is substantiated by numerical analyses, it may explain why the resistance of the HAs is lower than predicted by their radius (Fig. 3; Table 1). A more rigorous application of Poiseuille's Law will require the quantification of both radius and length of each artery and its branches.

The total peripheral resistance against which the heart must pump can be estimated by two independent techniques. The first is the reciprocal of the sum of the reciprocals of individual artery resistances as measured during perfusion (equation 2). The second method, based on the hydraulic resistance equation, is the mean ventricular pressure divided by $\dot{V}_b$. In the

first case, resistances measured are described as arising from the named artery, while in actuality the measurements relate to the total flow path including the sinuses leading back to the heart. The assumption is made that the resistance of the lacunar and venous sinuses is low relative to that of the arteries and their branches and that the sinuses do not therefore contribute to the differences between arteries. The latter assumption is justified because hemolymph from all arteries is collected into interconnected sinuses that should function as a unit (Burger and Smythe, 1953) and then returns to the heart through the branchial vessels. Thus, the 'venous' return portion of each artery is essentially common.

Reiber (1992), using a pulsed Doppler technique, measured the flow rate in each artery except the HAs in *H. americanus* (Table 1). Since Reiber found the flow rates for the SA and DAA were greater than our highest perfusion rates, we have estimated the individual arterial resistances by extrapolation of the data in Fig. 2 to the flow rates of Reiber to calculate an R_t of approximately 1.9 kPa s ml^{-1} (column 7, Table 1). If we use Reiber's flow values, making the assumption that each HA would have carried 3.8 ml min^{-1} (HAs make up 6.2 % of total arterial area), and our value of mean P_{vent}, we obtain an R_t of 0.93 kPa s ml^{-1} (column 6, Table 1, mean lobster mass 650±75 g).

These two resistance values can be compared with the R_t predicted from measurements of mean ventricular pressure and $\dot{V}_b$ of intact lobsters. An R_t of 0.77 kPa s ml^{-1} is obtained from the data of Burger and Smythe (1953) (a pulse pressure of 1.59 kPa yields a mean ventricular pressure of 0.86 kPa, equation 3, and $\dot{V}_b$ of 67 ml min^{-1} kg^{-1}). McMahon and Wilkens (1975) calculated $\dot{V}_b$ at 122 ml min^{-1} kg^{-1} using the Fick equation. Taking this value and the mean pulse pressure of intact lobsters from the present study yields an R_t of 0.53 kPa s ml^{-1}.

We do not know why the value for R_t derived from perfused arteries is double that obtained by other methods, but it appears that the flow resistance in intact animals may be lower than in our operated animals. Changing outflow in individual arteries does occur (McMahon, 1992), and this could be caused by the

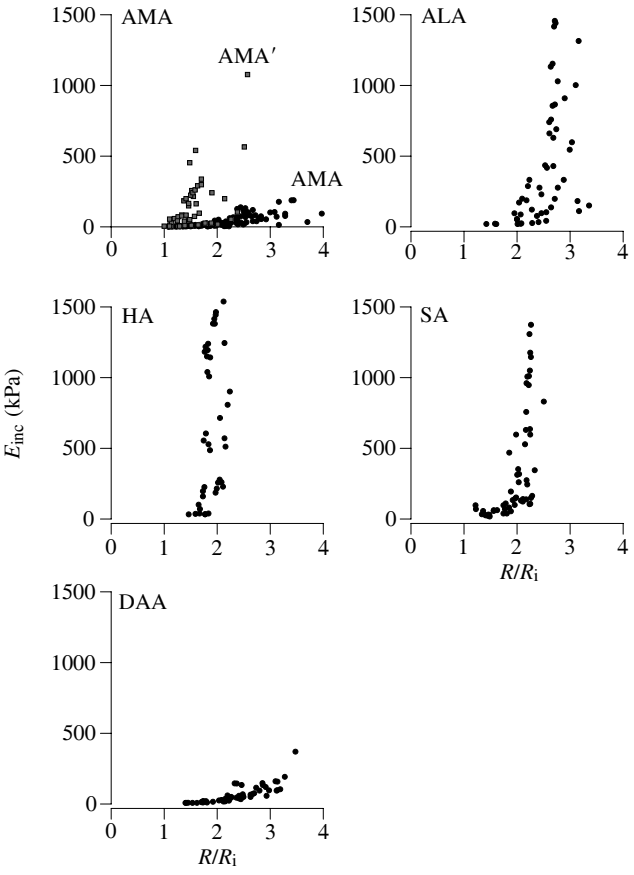

Fig. 7. The incremental modulus of elasticity (E_{inc}) of each artery type as a function of radius extension ratio (R/R_i) (N as in Fig. 5). Abbreviations are explained in the legend to Fig. 2.

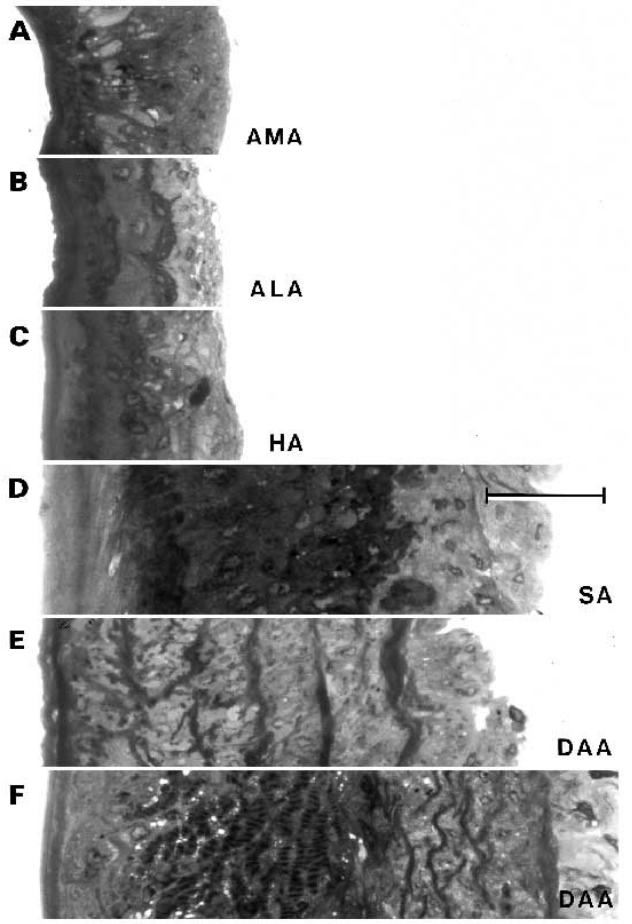

Fig. 8. Photomicrographs of transverse sections of the anterior median artery (A), anterior lateral artery (B), hepatic artery (C), sternal artery (D) and dorsal abdominal artery (E). Muscle fibers are apparent in the lateral walls of the dorsal abdominal artery (F). Variable amounts of adventitia appear at the outer borders of all vessels except the anterior median artery. Lumina appear on the left in the photomicrographs. Scale bar, 50 μm.

cardioarterial valves located at the origin of each artery (Kuramoto and Ebara, 1984; Kuramoto *et al.* 1992; Fujiwara-Tsukamoto *et al.* 1992; Wilkens *et al.* 1996) and by changes in arterial system resistance. In crayfish (Wilkens, 1995) and lobsters (Wilkens, 1997), the resistance to flow can be dramatically altered by adding neurotransmitters and neurohormones to the perfusion stream.

Although we cannot comment on the vascular impedance from our data, it is important to recall that the impedance to a pulsatile blood flow is lower than the resistance to a steady flow (Milnor, 1990). Impedance in the human aorta reaches a minimum at an oscillating frequency of 2–3 Hz. Thus, at resting heart rates of 1 Hz in lobsters, the impedance to flow will be lower than the steady flow resistances recorded here, and at elevated rates during exercise or stress it should be lower still. Counteracting the resistance-reducing effects of oscillatory flow will be the viscosity of hemolymph, which is 1.3 times that of saline (Maynard, 1960). Preliminary data indicate that the resistance to perfusion with saline when the viscosity is increased to 1.3 times that of the saline by adding 1.97 g l^{-1} polyvinyl pyrrolidone [M_r 1×10^6 to match that of hemocyanin (Mangum, 1983), Polysciences, Warrington, PA] is on average 1.5 times that when arteries are perfused with saline alone (G. W. Davidson and J. L. Wilkens, unpublished data).

Another way to test the validity of the present measurements is to calculate $\dot{V}_b$ from our measured values for pulse pressure and R_t. On the basis of a mean ventricular pressure (1.07 kPa) and R_t (1.93 kPa s ml^{-1}) at perfusion rates similar to *in vivo* flow rates, $\dot{V}_b$ would be 66 ml min^{-1} kg^{-1}. This is similar to the value of 67 ml min^{-1} kg^{-1} obtained by Burger and Smythe (1953) using the Fick equation.

When an autotomized lobster leg is flexed, hemolymph is extruded. This indicates that the volume of the appendage has decreased, and it raises the question of whether the resistance to flow might also be affected. During perfusion of the DAA, the abdomen was alternately pulled into an extended position and pushed into a flexed position. There is an overall tendency for the resistance to be higher when the abdomen is flexed, but the differences were significant only at low perfusion rates. The resistance does rise abruptly during active tail-flip flexions, but the increase only lasts for the period of movement (P. Lovell and J. L. Wilkens, unpublished observations on *Procambarus clarkii*).

Mechanical properties of arteries

The volume/pressure and radius extension ratio/pressure plots show that *H. americanus* arteries are compliant at radii close to their unpressurized radii, but all except the DAA become stiff at higher transmural pressures. At mean vascular pressures, most arteries will be relatively compliant. This agrees with recent data from Davison *et al.* (1995) for the DAA of *H. americanus*. The values of E_{inc} for lobster DAA and *C. magister* ALAs and SA recorded by Shadwick *et al.* (1990) are similar to the values for the same arteries recorded here. This suggests that the SA and ALAs of crabs must have similar mechanical properties to their homologs in the lobster.

Within the physiological range of hemolymph pressures that occur in lobsters, the compliance of all arteries predicts that each will function as a Windkessel, a simple elastic vessel emptying through a resistance that converts much of the pulsatile flow generated by the heart into a relatively steady flow to the periphery (Milnor, 1990). Recordings from the ALAs and DAA of intact lobsters confirm this prediction. The pulse pressures recorded from the DAA are about one-third of those produced by the heart (present observations; Belman, 1975).

There has been a general assumption that crustacean arteries lack muscle layers; however, striated muscle has been reported in the wall of the DAA of the spiny lobster *Panulirus interruptus* (Burnett, 1984), the prawn *Sicyonia ingentis* (Martin *et al.* 1989) and in *H. americanus* (Davison *et al.* 1995; present report). Since all *H. americanus* arteries other than the DAA lack muscle layers, they should behave as capacitance vessels rather than resistance vessels (Milnor, 1990). The role of muscle in the DAA is not known.

Histological examination provides a structural explanation for the greater compliance of the DAA relative to the other arteries. All arteries display a thick endothelium covered by fibrils. As these arteries expand, they will reach a point where the fibrillar lamina begins to be stretched, and at this point the E_{inc} would be expected to increase sharply. The DAA lacks a robust fibrillar lamina, but instead the lateral walls are supplied with striated muscle fibers. Photomicrographs of the DAA are similar to those published by Davison *et al.* (1995) and Martin and Hose (1995). It may be that the DAA relies on active regulation rather than indistensibility to control vessel diameter. If this proves to be the case, the DAA would be unique in possessing the properties of both capacitance vessels and resistance vessels.

We wish to thank Mr Darryl Gugleilmin for his assistance during the early stages of this project and Dr G. B. Bourne for helpful discussions. The histological sections of arteries used to measure wall thickness were prepared by Mr Michael White of the Foothills Hospital Histopathology Unit. Supported by the Student Temporary Employment Program of Alberta and Natural Sciences and Engineering Research Council of Canada (NSERC) operating grants to J.L.W. and by an operating grant from the President's NSERC Research Fund to M.J.C.

References

BELMAN, B. M. (1975). Some aspects of the circulatory physiology of the spiny lobster *Panulirus interruptus*. *Mar. Biol.* **29**, 295–305.

BERGEL, D. H. (1961). The static elastic properties of the arterial wall. *J. Physiol., Lond.* **156**, 445–457.

BERNE, R. M. AND LEVY, M. N. (1992). *Cardiovascular Physiology*, 6th edn, pp. 113–151. Toronto: Mosby Year Book.

BOURNE, G. B., JORGENSON, D. D., MCMAHON, B. R., BURNETT, L. E. AND DEFUR, P. L. (1988). An examination of cardiac performance in the dungeness crab *Cancer magister*. In *Society for Experimental Biology Proceedings*, Lancaster Meeting, (Abstract).

BURGER, J. W. AND SMYTHE, C. MCC. (1953). The general form of

circulation in the lobster *Homarus*. *J. cell. comp. Physiol*. **42**, 369–383.

BURNETT, B. R. (1984). Striated muscle in the wall of the dorsal abdominal aorta of the California spiny lobster *Panulirus interruptus*. *J. Crust. Biol*. **4**, 560–566.

CHANDRAN, K. B. (1992). *Cardiovascular Biomechanics*, pp. 94–137. New York: New York University Press.

COLE, W. (1941). A perfusing solution for the lobster (*Homarus*) heart and the effects of its constituent ions on the heart. *J. gen. Physiol*. **25**, 1–6.

DAVISON, I. G., WRIGHT, G. M. AND DEMONT, M. E. (1995). The structure and physical properties of invertebrate and primitive vertebrate arteries. *J. exp. Biol.* **198**, 2185–2196.

FUJIWARA-TSUKAMOTO, Y., KUWASAWA, K. AND OKADA, J. (1992). Anatomy and physiology of neural regulation of haemolymph flow in the lateral arteries of the isopod crustacean, *Bathynomus doederleini. Comp. Physiol*. **11**, 70–85.

GREENAWAY, P. AND FARRELLY, C. A. (1984). The venous system of the terrestrial crab *Ocypode cordimanus* (Desmarest 1825) with particular reference to the vasculature of the lungs. *J. Morph*. **181**, 133–142.

KURAMOTO, T. AND EBARA, A. (1984). Neurohormonal modulation of the cardiac outflow through the cardioarterial valve of the lobster. *J. exp. Biol*. **111**, 123–128.

KURAMOTO, T., HIROSE, E. AND TANI, M. (1992). Neuromuscular transmission and hormonal modulation in the cardioarterial valve of the lobster, *Homarus americanus*. *Comp. Physiol*. **11**, 62–69.

LOCKHEAD, J. H. (1950). Crayfishes (and *Homarus*). In *Selected Invertebrate Types* (ed. F. A. Brown, Jr), pp. 428–431. New York: John Wiley and Sons, Inc.

MANGUM, C. P. (1983). Oxygen transport in the blood. In *The Biology of Crustacea*, vol. 5, *Internal Anatomy and Physiological Regulation* (ed. L. H. Mantel), pp. 373–439. New York: Academic Press.

MARTIN, G. G. AND HOSE, J. E. (1995). Circulation, the blood and disease. In *Biology of the Lobster* Homarus americanus (ed. J. R. Factor), pp. 465–495. New York: Academic Press.

MARTIN, G. G., HOSE, J. E. AND CORZINE, C. J. (1989). Morphological comparison of major arteries in the ridgeback prawn, *Sicyonia ingentis*. *J. Morph*. **200**, 175–183.

MAYNARD, D. M. (1960). Circulation and heart function. In *The Physiology of Crustacea*, vol. 1, *Metabolism and Growth* (ed. T. H. Waterman), pp. 161–226. New York: Academic Press.

MCLAUGHLIN, P. A. (1983). Internal anatomy. In *The Biology of Crustacea*, vol. 5, *Internal Anatomy and Physiological Regulation* (ed. L. H. Mantel), pp. 1–52. New York: Academic Press.

MCMAHON, B. R. (1992). Factors controlling the distribution of cardiac output in decapod crustaceans. *Comp. Physiol*. **11**, 51–61.

MCMAHON, B. R. AND BURNETT, L. E. (1990). The crustacean open circulatory system: A reexamination. *Physiol. Zool*. **63**, 35–71.

MCMAHON, B. R. AND WILKENS, J. L. (1975). Respiratory and circulatory responses to hypoxia in the lobster *Homarus americanus*. *J. exp. Biol*. **62**, 637–655.

MCMAHON, B. R. AND WILKENS, J. L. (1983). Ventilation, perfusion and oxygen uptake. In *The Biology of Crustacea*, vol. 5, *Internal Anatomy and Physiological Regulation* (ed. L. H. Mantel), pp. 289–372. New York: Academic Press.

MILNOR, W. R. (1990). *Cardiovascular Physiology*, pp. 171–218. Oxford: Oxford University Press.

REIBER, C. L. (1992). The hemodynamics of the crustacean open circulatory system: Hemolymph flow in the crayfish (*Procambarus clarkii*) and the lobster (*Homarus americanus*). PhD thesis, University of Massachusetts, Amherst.

REIBER, C. L. (1994). Hemodynamics of the crayfish *Procambarus clarkii*. *Physiol. Zool.* **67**, 449–467.

RICHARDSON, K. C., JARETT, L. AND FINKE, E. H. (1960). Embedding in epoxy resins for ultrathin sectioning in electron microscopy. *Stain Technol*. **35**, 313–323.

SHADWICK, R. E., POLLOCK, C. M. AND STRICKER, S. A. (1990). Structure and biomechanical properties of crustacean blood vessels. *Physiol. Zool*. **63**, 90–101.

WILKENS, J. L. (1995). Regulation of the cardiovascular system in crayfish. *Am. Zool*. **35**, 37–48.

WILKENS, J. L. (1997). Possible mechanisms of vascular resistance in the lobster *Homarus americanus. J. exp. Biol*. **200**, 487–493.

WILKENS, J. L., KURAMOTO, T. AND MCMAHON, B. R. (1996). The effects of six pericardial hormones and hypoxia on the semi-isolated heart and sternal arterial valve of the lobster *Homarus americanus*. *Comp. Biochem. Physiol.* **114**C, 57–65.

WILKENS, J. L. AND MCMAHON, B. R. (1994). Cardiac performance in semi-isolated heart of the crab *Carcinus maenas*. *Am. J. Physiol.* **266**, R781–R789.

WILKENS, J. L. AND YOUNG, R. E. (1992). Regulation of pulmonary blood flow and the blood pressure in a mangrove crab (*Goniopsis cruentata*). *J. exp. Biol*. **163**, 297–316.